Engineering Failure Analysis 16 (2009) 1245–1251

Contents lists available at ScienceDirect

Engineering Failure Analysis

journal homepage: www.elsevier.com/locate/engfailanal

Fracture toughness of the heat affected zone on Nd-YAG laser welded joints

J.M. Costa [a,*], J.M. Ferreira [a], C. Capela [b]

[a] CEMUC, Department of Mechanical Engineering, University of Coimbra – Polo II, Pinhal de Marrocos, 3030-788 Coimbra, Portugal
[b] Centre for Rapid and Sustainable Product Development, Polytechnic Institute of Leiria, INDEA (Campus 5), Rua das Olhalvas, 2414-016 Leiria, Portugal

ARTICLE INFO

Article history:
Received 21 July 2008
Accepted 1 August 2008
Available online 19 September 2008

Keywords:
Mould producing
Laser repairing
Welded joints
Fracture toughness

ABSTRACT

Laser deposit welding based on modern Nd-YAG lasers is a new mould repair process with advantages relatively to the traditional methods (Micro-plasma and TIG methods). For moulds steels there are no research studies about the laser deposit welding process effects in respect to fracture toughness, hardness and residual stresses variations in the laser-deposited layer and in the heat affected zone. These variations will have an important influence in the thermal–mechanical fatigue strength of the moulds parts. This paper is concerned on the study of the fracture toughness of transient microstructure regions in Nd-YAG laser welded joints performed in mould steels. Fracture toughness tests were performed in two hot-working tool steels: AISI H13 and AISI P20. Small welded specimens were prepared with U notches and filled with laser welding deposits. The hardness profiles were obtained at the middle cross-section of specimens against distance to the surface in order to identify the microstructures present at the crack tip region. Fracture toughness was evaluated and plotted against the Vickers hardness measured at the fatigue crack tip. Depending of the crack tip depth two very different toughness levels were observed in the H13 steel, while a lower variation of toughness was observed for the P20 steel. The values of fracture toughness observed in each specimen are consistent with the correspondent crack tip microstructure hardness.

1. Introduction

Mould producing manufacturing is usually extremely exact and consequently very expensive. Therefore, repair techniques for the correction of localized imperfections due to design or/and execution imperfections during moulds manufacturing as well as tool marks are very important. Laser deposit welding, by using modern ND-YAG lasers, is a new repair process, very flexible, that have the advantage relatively to the traditional methods of achieving less change of the metal composition around the repair zone. Moreover, it permits a very accurate deposition of a small volume of the filler material to the area chosen at the work-piece surface, with low distortion.

X.40.CrMoV.5.1 (AISI H13) and 40.CrMnNiMo.8.6.4 (AISI P20) are two hot-working tool steels largely used in Portuguese industry moulds production. Because of its excellent combination of high toughness and resistance to thermal fatigue cracking H13 is used for more hot work tooling applications. P20 mould steel is a versatile, low-alloy tool steel that is characterized by good toughness at moderate strength levels. However, for these steels there are no research studies about the laser deposit welding process effects in respect to fracture toughness, hardness and residual stresses variations in the laser-deposited layer and in the heat affected zone. These variations will have an important influence in the thermal–mechanical fatigue strength of the moulds parts.

* Corresponding author. Fax: +351 239790701.
E-mail address: jose.domingos@dem.uc.pt (J.M. Costa).

1350-6307/$ - see front matter
doi:10.1016/j.engfailanal.2008.08.002

In a previous work [1–3], the authors observed that welded specimens, tested at $R = 0.4$, presented a similar fatigue resistance to the correspondent non-welded specimens tested for the same stress ratio and also very close to the curve obtained with welded specimens for $R = 0$. Measurement with two complementary techniques proves that residual stresses are the main factor to explain that fatigue behaviour [3]. The present study have the aim of to complement previous work in the characterization of the laser welded deposits. Therefore, this paper is concerned on the study of the fracture toughness of transient microstructure regions in Nd-YAG laser welded joints performed in these two mould steels. The hardness profiles will be obtained in order to identify the microstructures present at the specimens fatigue crack tip. Fracture toughness was evaluated and plotted against the Vickers hardness measured at the fatigue crack tip.

2. Experimental

This paper presents the experimental results of fracture toughness evaluation in laser welding deposits performed in two hot-working tool steels: AISI H13 and AISI P20. The chemical composition and the main mechanical properties of these alloys are shown in Tables 1 and 2, respectively. A Nd-YAG laser process was used in order to simulate the repair of damaged tool

Table 1
Chemical composition of the analysed steels (weight%)

Mould steel		C	Si	Mn	Cr	Mo	Ni	V
DIN	AISI							
X.40.CrMoV.5.1	H13	0.39	1.0	0.4	5.2	1.3	–	1.0
40.CrMnNiMo.8.6.4	P20	0.37	0.3	1.4	2.0	0.2	1.0	–

Table 2
Mechanical properties of the mould steels

Mould steel		Tensile strength, σ_{UTS} (MPa)	Yield strength, σ_{YS} (MPa)	Elongation, ε_r (%)	Hardness (HV)
DIN	AISI				
X.40.CrMoV.5.1	H13	1990	1650	9	550
40.CrMnNiMo.8.6.4	P20	995	830	12	350

Table 3
Chemical composition of the filler material (weight%)

	C	Si	Mn	Cr	Mo	Ni	V	Fe
H13	0.15	1.5	2	20	–	7	–	Rest.
P20	0.25	–	1.4	1.6	0.3	–	0.4	Rest.

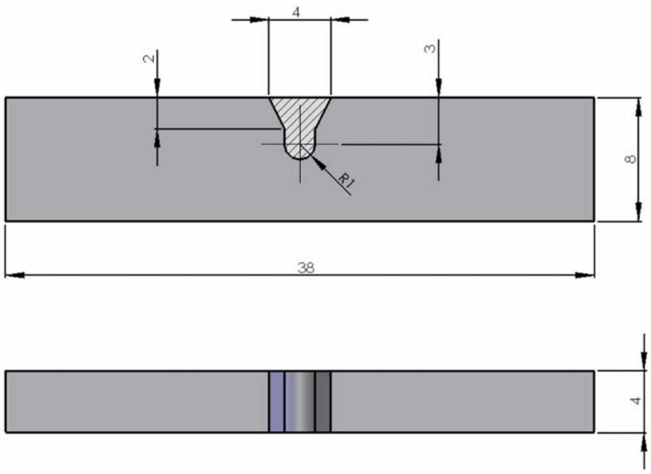

Fig. 1. Geometry of fracture toughness specimens.

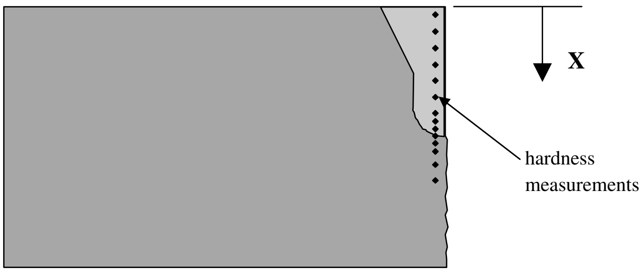

Fig. 2. Schematic illustration of hardness measurements locali.

surfaces. Welding was conduced with an Nd-YAG laser system, HTS 180 Laser Tool, using a pulsating electric current with 6 Hz and 8 ms of impulse time. A filler wire with 0.4 mm diameter was used. The power was 63% of the maximum power (180 W), with a laser diameter of 0.6 mm. The chemical compositions of the filler materials are presented in Table 3. An Air/He-mixture (5% He) with a flow of 0.6 l/min was used as shielding gas. After the conclusion of the laser deposit welding operation, the specimens were grinded to obtain a homogeneous specimen thickness. Welded specimens were prepared with U notches and filled with laser welding deposits. Fig. 1 illustrates the major dimensions of the samples used in the tests. The radius of the U notch was 0.5 mm. Several laser-deposited layers were performed. Fatigue bending testes were carried out in order to produce fatigue pre-cracks with its tip localized near or into the heat affected zone.

In order to characterize the welded joint and the heated affected zone (HAZ) Vickers hardness profiles were obtained using a Struers Type Duramin-1 microhardness tester, with an indentation load of 500 gf during 15 s, according to the ASTM E 348 standard [4]. The hardness profiles were obtained at the middle thickness surface, close to the fracture surface border as illustrated in Fig. 2.

Fracture toughness results were discussed taken in account complementary parameters, such as: the hardness profiles, microstructures of failure zone, size of melted material and pre-crack. Fracture toughness was evaluated according BS 7448:91 [5].

3. Results

Fig. 3 shows hardness values against distance to the specimen surface (see Fig. 2) for both steels. From H13 steel hardness profile it was concluded that the filler material has a significant lower hardness than the parent material and that the thermal effects of the welding laser process induce a slight material hardening in the HAZ and that this zone is very narrow: a minimum of 250 HV was obtained in the filler material and a maximum of 680 HV in the HAZ. The P20 steel hardness profile has a very different aspect: the parent material has a hardness of about 350 HV while the HAZ has a maximum of 540 HV. The chemical composition of the fillers used for welding the two steel specimens is the main factor to explain the different hardness profiles observed.

In Fig. 4 the hardness values at the fatigue crack tip were determined for each specimen, plotting partially the hardness curves of Fig. 3 and the effective crack length of each specimen.

Table 4 summarizes all data concerning fracture toughness tests. All criteria of rejection included in the BS 7448:91 standard were considered for the validation of the fracture tests. Two types of load–displacement plots were obtained

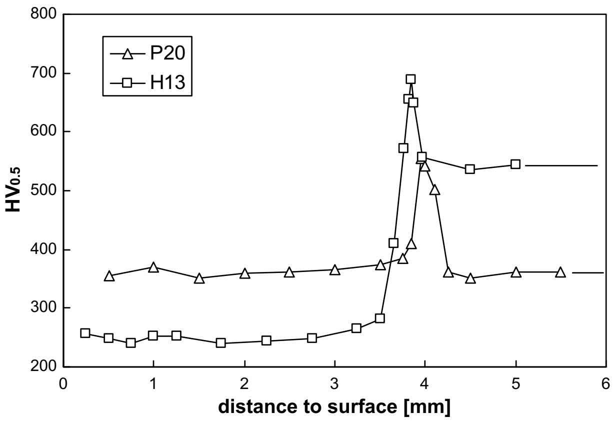

Fig. 3. Hardness profiles in laser welded specimens for fract.

depending of both material type and localization of the fatigue crack tip relatively to the heat affected zone, Fig. 5a and b. For P20 steel the plot type III was always obtained independently of the fatigue crack length. For this steel only K_Q values can be reported because no valid values of K_{Ic} were obtained. The criterion not met is indicate in Table 4. Therefore, the test data were re-analysed in order to calculate the J_{Ic} parameter. For the H13 steel the type I plot was observed with different maximum loads depending on the crack tip hardness. When fatigue crack tip was localized into the harder heat affected zone the type I load–displacement plot attain lower load values. For the specimens with the crack tip outside the heat affected zone the load–displacement plot is characterized by much higher load values. In this case the fatigue crack has its tip near the HAZ but remaining into the filler material or into the base material with lower values of hardness.

In order to understand the influence of the transient microstructures near the heat affected zone produced by the laser welded deposit, fracture toughness values were plotted against the hardness measured at the fatigue crack tip region for both steels in Fig. 6. We can observe that fracture toughness obtained in each specimen is consistent with the correspondent microstructure hardness: as microstructure hardness increases the fracture toughness decreases. H13 steel shows a large range of K_Q, K_{Ic} values between 38 and 124 MPa m$^{0.5}$ due to the also large range of microstructure hardness between 520 and 670 $HV_{0.5}$. Valid K_{Ic} values were obtained for the specimen where the crack tip have higher values of hardness, as indicated in Fig. 6a. In the case of P20 steel Fig. 6b shows a slight decreases of fracture tough-

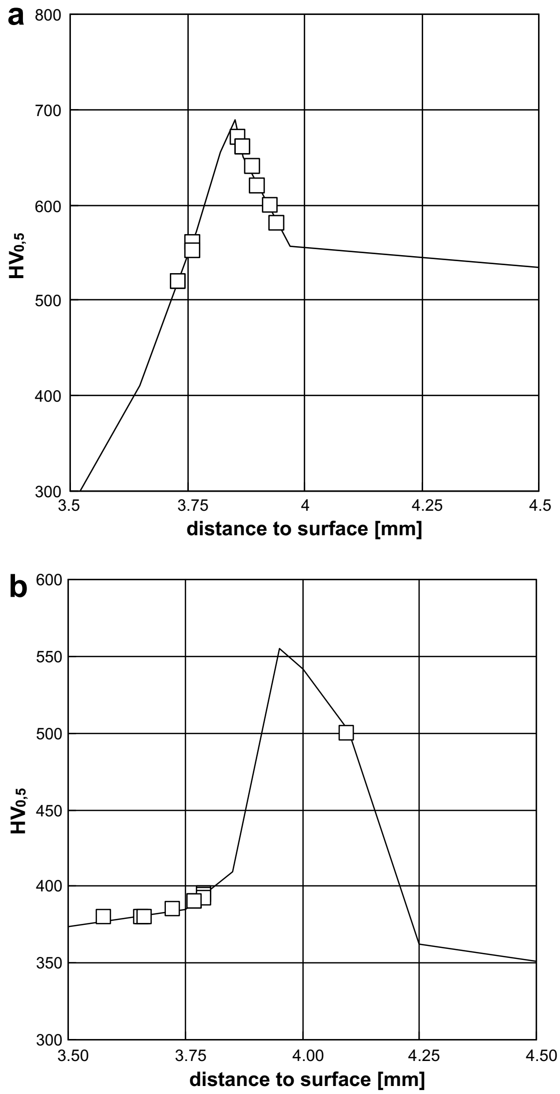

Fig. 4. Hardness values at the fatigue crack tip: (a) H13 spec, and (b) P20 spec.

Table 4
Fracture toughness test results in P20 and H13 moulds

Specimen number	a (mm)	P_Q (N)	K_Q (MPa $m^{0.5}$)	$HV_{0.5}$	$2.5*(K_Q/\sigma_{ys})^2$	W–a	F_{max}/F_d	J_m (J/mm^2)	Valid K_{Ic}?
P20-01	3.66	3544	88.7	380	28.5	4.34	1.13	170	No
P20-02	3.72	3205	82.2	385	24.5	4.28	1.22	169	No
P20-03	3.66	3130	78.8	380	22.5	4.34	1.26	222	No
P20-04	4.10	2698	80.4	500	23.4	3.90	1.01	48	No
P20-05	3.66	3219	80.1	380	23.3	4.34	1.13	132	No
P20-06	3.79	3210	83.0	395	25.0	4.21	1.11	162	No
P20-07	3.77	3350	87.9	390	28.1	4.23	1.15	218	No
P20-08	3.79	3050	79.9	394	23.2	4.21	1.14	138	No
P20-09	3.79	3328	85.4	392	26.5	4.21	1.09	152	No
P20-10	3.77	3290	83.9	390	25.5	4.23	1.15	170	No
P20-11	3.58	3230	78.6	380	22.4	4.42	1.15	205	No
H13-01	3.73	4800	121.5	520	13.6	4.54	1.01	65	No
H13-02	3.76	4548	116.2	560	12.4	4.49	1.00	58	No
H13-03	3.93	3500	93.2	600	8.0	4.38	1.00	38	No
H13-04	3.89	1638	44.1	640	1.8	4.37	1.01	8	yes
H13-05	3.86	1592	42.4	670	1.7	4.40	1.00	8	yes
H13-06	3.87	1401	38.3	660	1.3	4.30	1.00	6	yes
H13-07	3.87	1296	35.8	660	1.2	4.30	1.00	6	yes
H13-08	3.90	2832	76.0	620	5.3	4.37	1.00	25	No
H13-09	3.76	4858	124.1	552	14.1	4.50	1.00	67	No
H13-10	3.73	4467	110.0	520	11.1	4.61	1.00	52	No
H13-11	3.94	4085	110.7	580	11.3	4.34	1.00	53	No

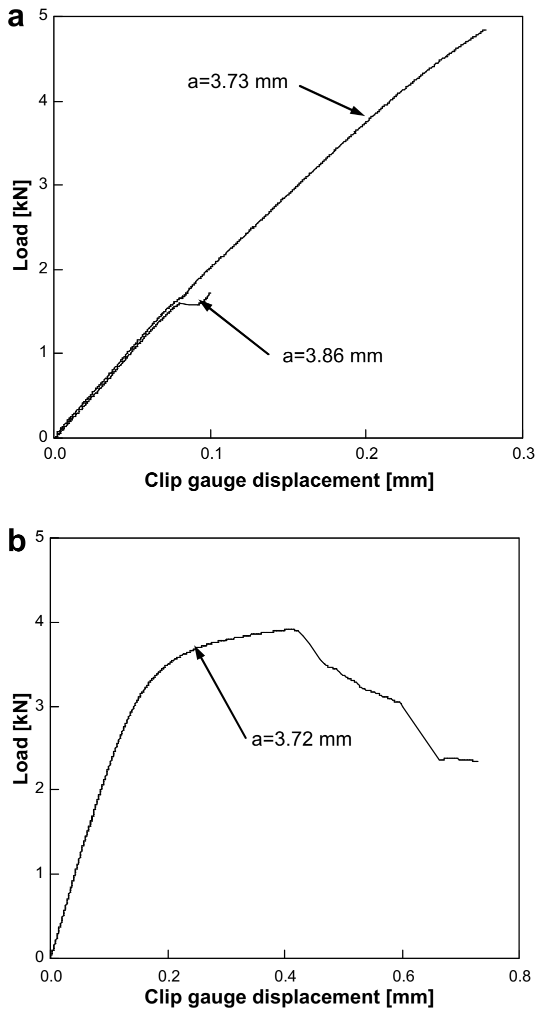

Fig. 5. Typical load–displacement plots: (a) H13 specimens, and (b) P20 specimens.

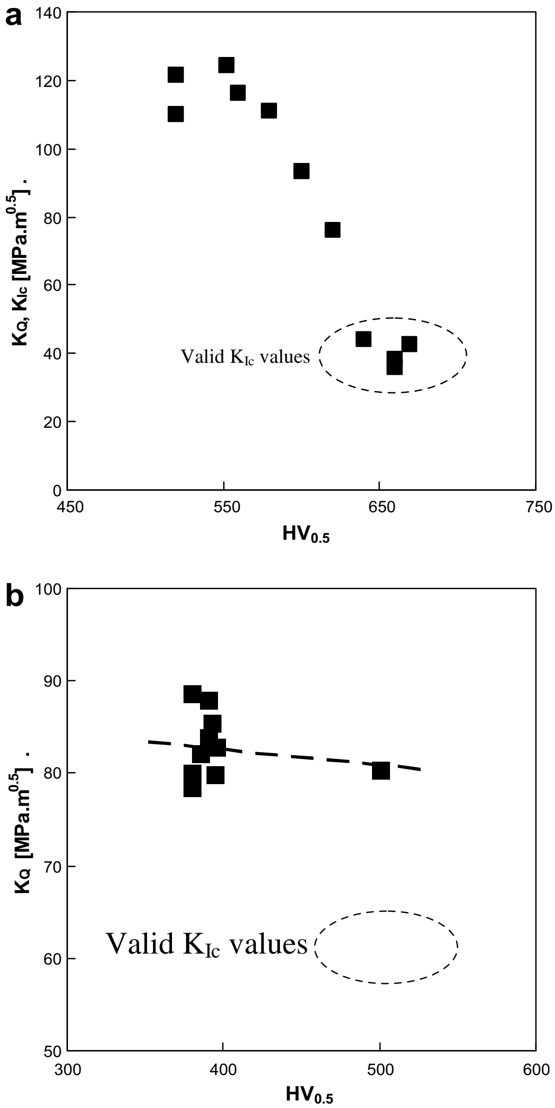

Fig. 6. Fracture toughness against microstructure hardness near the crack tip: (a) H13 spec, and (b) P20 spec.

ness K_Q with the increases of hardness in the range 380–500 $HV_{0.5}$. P20 steel have a range of microstructures more uniform with a lower variation of hardness due the chemical compositions of both filler and base materials are more similar than in the case of H13 steel. No valid K_{Ic} values were obtained for this steel with the specimen geometry used.

Fig. 7 presents the fracture toughness parameter J_m against microstructure hardness at fatigue crack tip for the P20 steel. A greater scatter band of fracture toughness values was obtained. This is a expected behaviour due J Integral parameter also consider the plastic energy until maximum load. We can also observe a greater sensitivity of this parameter with the microstructure hardness of the fatigue crack tip.

The results obtained in this work, specially with H13 steel, show that even in the case of parts repaired by laser depositing welding, imposing a very narrow heat affected zone, the fracture toughness can present a greater variation due the transient microstructures observed into the heat affected zone. Tanking into account that moulds steels are subjected to strong thermo-mechanical loads, especially in the case of the aluminium die castings, the damage of the moulds surface in the form of wear or fatigue cracks can occur. The subsequent propagation of a fatigue crack can result in a final fracture when the crack tip attain these lower fracture toughness structures if the maximum stress intensity factor of the loading cycle is higher enough to attain the critical value of the fracture toughness parameter. Therefore, fracture assessment based on parent material properties is incorrect and on the none-conservative side.

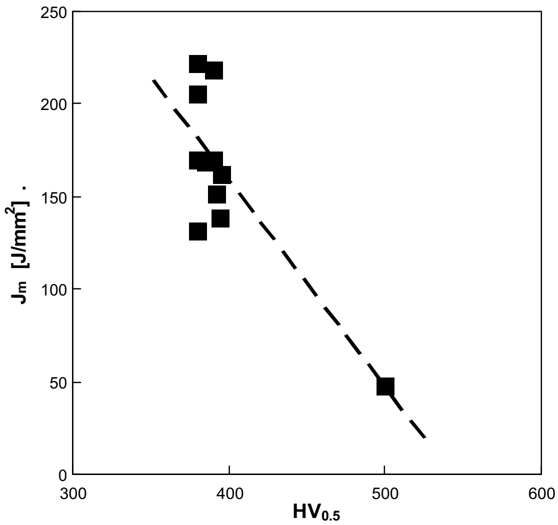

Fig. 7. Fracture toughness J_m against microstructure hardness.

4. Conclusions

H13 steel hardness profile shows that the thermal effects of the welding laser process induce a significant material hardening in a very narrow HAZ with a maximum hardness of 680 HV. The P20 steel hardness profile has a very different aspect: the filer and parent material have a hardness of about 350 HV while the HAZ has a maximum of 540 HV. The chemical composition of the fillers used for welding the two steel specimens is the main factor to explain the different hardness profiles observed.

The results obtained in this work, specially with H13 steel, show that even in the case of parts repaired by laser depositing welding, imposing a very narrow heat affected zone, the fracture toughness can present a greater variation due the transient microstructures observed into the heat affected zone. Therefore, fracture assessment based on parent material properties is incorrect and on the none-conservative side.

Acknowledgments

The authors would like to acknowledge POCI programme, Project POCI/EME/55918/2004, for funding the work reported and Anibal H. Abrantes S.A. company for performing the laser welds.

References

[1] Borrego LP, Pires JTB, Costa JM, Ferreira JM. Fatigue behaviour of laser repairing welded joints. Eng Failure Anal 2007;14(8):1586–93.
[2] Borrego LP, Pires JTB, Costa JM, Ferreira JM. Moulds repaired by laser welding. Eng Failure Anal 2008. doi:10.1016/j.engfailanal.2008.02.010.
[3] Costa JM, Pires JTB, Antunes VF, Nobre JP, Borrego LP. Residual stresses analysis of Nd-YAG laser welded joints. In: XXV Encuentro del Grupo Español de Fractura, Siguenza, 5–7 de Março de; 2008. p. 403–8.
[4] American society for testing and materials. Standard test method for microhardness of materials. Annual book of ASTM standards, vol. 03.01. ASTM E 384; 2000.
[5] BS 7448:91, Fracture mechanics toughness methods tests: part 1: methods for determination of K_{IC}, critical CTOD and critical J values of metallic materials. British Standards Institution; 1991.